METHODS

Human Mutation

OFFICIAL JOURNAL HGVS HUMAN GENOME VARIATION SOCIETY www.hgvs.org

Assessing High-Resolution Melt Curve Analysis for Accurate Detection of Gene Variants in Complex DNA Fragments

Elizabeth A. Tindall,[1–3] Desiree C. Petersen,[1,2] Paula Woodbridge,[1,2] Katharina Schipany,[2] and Vanessa M. Hayes[1–3]*

[1]*Cancer Genetics Group, Children's Cancer Institute Australia for Medical Research, Sydney Children's Hospital, Randwick, Sydney, NSW, Australia;* [2]*Cancer Genetics Group, Cancer Research Program, Garvan Institute of Medical Research, St. Vincent's Hospital, Darlinghurst, Sydney, NSW, Australia;* [3]*University of New South Wales, Sydney, NSW, Australia*

For the Focus Section on HRMA Technology

Received 16 June 2008; accepted revised manuscript 10 September 2008.
Published online 11 March 2009 in Wiley InterScience (www.interscience.wiley.com). DOI 10.1002/humu.humu.20919

ABSTRACT: Mutation detection has, until recently, relied heavily on the use of gel-based methods that can be both time consuming and difficult to design. Nongel-based systems are therefore important to increase simplicity and improve turn around time without compromising assay sensitivity and accuracy, especially in the diagnostic/clinical setting. In this study, we assessed the latest of the nongel-based methods, namely high-resolution melt (HRM) curve analysis. HRM is a closed-tube method that incorporates a saturating dye during DNA amplification followed by a monitoring of the change in fluorescence as the DNA duplex is denatured by an increasing temperature. We assessed 10 amplicons derived from eight genes, namely *SERPINA1*, *CXCR7*, *MBL*, *VDR*, *NKX3A*, *NPY*, *TP53*, and *HRAS* using two platforms, the LightScanner® System using LC Green® PLUS DNA binding dye (Idaho Technology, Salt Lake City, UT, USA) and the LightCycler® 480 using the HRM Master dye (Roche Diagnostics, Indianapolis, IN, USA). DNA variants (mutations or polymorphims) were previously identified using denaturing gradient gel electrophoresis (DGGE) a method, similarly to HRM, based upon the different melting properties of double-stranded DNA. Fragments were selected based on variant and fragment complexity. This included the presence of multiple sequence variants, variants in alternate orientations, and single or multiple variants (constitutional or somatic) in GC-rich fragments. We demonstrate current limitations of the HRM method for the analysis of complex DNA regions and call for caution when using HRM as the sole method to make a clinical diagnosis based on genetic analysis.
Hum Mutat 30, 876–883, 2009 © 2009 Wiley-Liss, Inc.

KEY WORDS: mutation detection; high resolution melt; HRM; LightScanner; LightCycler; denaturing gradient gel electrophoresis; DGGE; Multiple Variants; GC-rich

Introduction

The contribution of DNA sequence variation to human disease and individual response to treatment is well documented. The availability of rapid, efficient, and reliable technologies for genetic-based testing is therefore critical for clinical and prenatal diagnostics, patient management, predisposition testing, and pharmacogenetics. Although the research community can afford a small degree of error, mutation screening in a diagnostic laboratory must be near 100% for both sensitivity and specificity.

Despite being the only direct approach for mutation detection, Sanger dideoxy sequencing has, to date, been considered an inappropriate method based on the high cost associated with it. Recent advances in high-throughput sequencing include 454-sequencing (Roche, Basel, Switzerland; www.roche.com), which applies the principles of pyrosesquencing [Margulies et al., 2005], Illumina-sequencing (formerly Solexa, Illumina, Inc., San Diego, CA, USA; www.illumina.com) based on single base extension [Bentley, 2006], SOLiD™ System (Applied Biosystems [ABI], Foster City, CA, USA; www.appliedbiosystems.com) using sequencing by ligation, and more recently, true Single Molecule Sequencing™ (tSMS™) (Helicos Bioscience corp., Cambridge, MA, USA; www.helicosbio.com), which is similarly a sequencing-by-synthesis approach that uses single DNA molecules to generate a sequence. Although next generation sequencing technologies hold the potential to improve throughput and cost up to 100-fold, they are still costly and currently unrealistic alternatives for diagnostic laboratories [Schuster, 2008]. To date, the common approach to mutation detection is to use prescreening methods to identify specific regions of sequence variation, thus reducing the amount of direct sequencing required. Older methods that require post-PCR separation by gel electrophoresis include, denaturing gradient gel electrophoresis (DGGE) [Fischer and Lerman, 1983], temperature gradient gel electrophoresis (TGGE) [Rosenbaum and Riesner, 1987], chemical cleavage of mismatch (CCM) [Cotton et al., 1988], single-strand conformational polymorphism (SSCP) [Orita et al.,

Additional Supporting Information may be found in the online version of this article.

*Correspondence to: Dr. Vanessa M. Hayes, Cancer Genetics Group, Children's Cancer Institute Australia, Level 2, 66 High Street, Randwick, NSW 2031, Australia. E-mail: vhayes@ccia.unsw.edu.au

1989], confirmation sensitive gel electrophoresis (CSGE) [Ganguly et al., 1993], and heteroduplex analysis (HA) [Highsmith et al., 1999]. These gel-based systems remain the predominant methods of choice in diagnostic laboratories around the world. Our laboratory has routinely used DGGE and the Ingeny PhorU system (Ingeny, Goes, The Netherlands; www.ingeny.com) for highly sensitive de novo presequencing mutation detection. It is essential, however, that nongel-based, automated systems are developed not only to achieve more rapid results, but more importantly to reduce hands-on time and the level of technical expertise required. Two of the most commonly used nongel-based technologies include denaturing high-performance liquid chromatography (dHPLC) [Xiao and Oefner, 2001], and more recently, high-resolution melt (HRM) curve analysis [Wittwer et al., 2003].

HRM curve analysis is a closed-tube assay, introduced as a means of mutation scanning without the requirement of any post-PCR handling. A saturating DNA binding dye is introduced during DNA amplification, which enables differentiation of PCR products based on their dissociation behavior as they are subjected to increasing temperatures [Poláková et al., 2008]. In this study, we refer to two platforms for HRM curve analysis, the LightScanner® System using the LC Green® PLUS DNA binding dye (Idaho Technology) and the LightCycler® 480 using the HRM Master dye (Roche Diagnostics Corporation, Indianapolis, IN, USA). Unlike the previously described SYBR® Green I detecting dye, used for low resolution sequence analysis [Papp et al., 2003; Ririe et al., 1997], LC Green® PLUS and HRM Master dye can be used at saturating concentrations without inhibiting amplification [Grievink and Stowell, 2008; Wittwer et al., 2003], aiding to enhance assay sensitivity. LC Green® PLUS, however, has been found to increase the melting temperature of primers [Laurie et al., 2007], while the HRM Master dye does not have this effect. Using the LightScanner® System Call-IT® and LightCycler® 480 Gene Scanning software, heterozygous samples are identified by a change in the melt curve shape, achieved by plotting the fluorescence difference between melt curves compared to the reference (usually the wild-type) profile. Amplification of heterozygous samples produces both low melting heteroduplexes and high melting homoduplexes, which results in a skewed melt curve [Laurie et al., 2007; Wittwer et al., 2003].

In this study, we evaluate HRM curve analysis for detection of mutations previously identified using DGGE. DGGE is similarly based upon the different melting properties of double-stranded DNA. In short, amplified DNA is electrophoresed through an increasing gradient of denaturants, urea, and formamide (UF), at a fixed elevated temperature [Fischer and Lerman, 1983]. To facilitate mutation detection, a GC-rich fragment (GC-clamp) is introduced during amplification [Abrams et al., 1990; Myers et al., 1985; Sheffield et al., 1989]. Heteroduplexing results in the formation of mismatched heteroduplex bands, allowing for easy visualization of heterozygous sequence variation. The success of DGGE is, however, highly dependent on the choice of primers, including GC-clamp location [Wu et al., 1998] and gel conditions [Hayes et al., 1999].

With the demand for diagnostic based genetic testing on the rise, evaluation of more rapid, reliable, and cost-effective methods of mutation detection is crucial. In this analysis of one of the most recent of these methods, we are particularly concerned about the ability of HRM curve analysis to detect multiple sequence variants (both constitutional and somatic) within single fragments, as well as detecting variants within GC-rich regions, known to be problematic for almost any mutation detection method. Using these criteria, DNA variants were previously identified in 10 selected amplicons from eight genes using DGGE.

Materials and Methods

Amplicons Analyzed

All amplicons assessed in this study were initially screened for mutations via DGGE and selected for comparison with HRM curve analysis based on variant frequency, orientation, or GC content. No other selection bias was used. The 10 fragments screened in this study were derived from eight genes with amplicon sizes and primers depicted in Supp. Table S1. These include regions in intron 1 and exon 3 (including splice junctions) of the gene encoding for Alpha-1 Antitrypsin (*SERPINA1*; alternative names: *PI1*, and *AAT*; MIM# 107400; GenBank NM_000295.4) (DGGE assay) [Hayes, 2003], a region in exon 2 of the gene encoding CXC Chemokine Receptor 7 (*CXCR7*; alternative names: *CMKOR1*, *GPR159*, and *RDC1*; MIM# 610376; GenBank NM_020311.2), a region in exon 1 of the gene encoding for Mannose Binding Lectin (*MBL*; alternative names: *MBL2, MBP1,* and *COLEC1*; MIM# 154545; GenBank NM_000242.2), a region spanning exon 2 (including splice junctions) of the gene encoding for the Vitamin D Receptor (*VDR*; MIM# 601769; GenBank NM_000376.2) (DGGE assay) [Hayes et al., 2005], a region encompassing exon 1 of the Homeobox 3A gene (*NKX3A* or *NKX 3.1*; MIM# 602041; GenBank NM_006167.2), a region in exon 2 of Neuropeptide Y (*NPY*; MIM# 162640; GenBank NM_000905.2), two fragments within exon 4 and exon 5 of the gene for Tumour protein p53 (*TP53*; alternative names *P53* and *TRP53*; MIM# 191170; GenBank NM_000546.4), and a region within exon 2 of the Harvey rat sarcoma viral oncogene (*HRAS* or *HRAS1*; MIM# 190020; GenBank NM_005343.2). Regions assessed were identical for the DGGE and HRM methods, with the exception of the *SERPINA1* exon 3 region where a slightly shorter HRM amplicon was used.

Denaturing Gradient Gel Electrophoresis

In our laboratory, DGGE was the standard method of choice for comprehensive sequence analysis. The amplicons in this study were screened as part of alternative projects, where the aim was to detect all possible sequence variation. Study numbers ranged from 110 to 1,982 samples for constitutional DNAs, whereas the study numbers ranged from 25 to 100 for somatic variant detection.

DGGE primers were designed using the melt 87 computer program [Lerman and Silverstein, 1987] and following conditions for selecting optimal PCR fragments and primers as outlined by Wu et al. [1998]. A 40-bp GC fragment was added to the 5′ end of one of the DGGE primers to prevent total strand dissociation during denaturation, while an additional GC stretch was added to selected primers to achieve a single melt domain [Wu et al., 1998] (Supp. Table S1). Primers were synthesized at Integrated DNA Technology (IDT, Coralville, IA, USA).

A 25 µl PCR included at least 25 ng of genomic DNA, 0.1 mM of each deoxyribonucleotide triphosphate (dNTP), 10 pmol of each primer, 2.5 mM of a 10 × Mg^{2+} reaction buffer and 0.5 units of DNA Taq polymerase (Roche). PCR cycling conditions were as follows: an initial denaturation at 96°C for 3 min, followed by 32 cycles of denaturation at 96°C for 45 sec, annealing for 1 min (annealing temperatures shown in Supp. Table S1) and elongation at 72°C for 1 min 20 sec. The last cycle was followed by an additional extension step at 72°C for 7 min. Following amplification, a heteroduplexing step, which included denaturation at 96°C for 10 min, and renaturation at the annealing temperature (Supp. Table S1) for 45 min, was applied for optimal DGGE analysis.

DGGE conditions were optimized by considering improvements previously described by Hayes et al. [1999] and performed

using the INGENYphorU® system. Nine of the amplicons were electrophoresed through a 9% polyacrylamide gel containing an increasing gradient of UF optimized for each fragment, while the *NPY* amplicon was electrophoresed through a polyacrylamide gel ranging from 9 to 12% with an increasing UF gradient (Supp. Table S1). The gels for five amplicons derived from four genes (*SERPINA1*, *CXCR7, MBL,* and *VDR*) were run overnight at a constant elevated temperature of 60°C and 110 volts. DGGE conditions for the remaining five amplicons, which we describe as having a high GC content (ranging from 65% to 72.5%), derived from four genes (*NKX3A, NPY, TP53,* and *HRAS*), were optimized by running time travel gels [Myers et al., 1987]. Variant detection was optimal at specific time points ranging between 6 and 7.5 hr at a constant temperature of 60°C and 150 volts. The gels were stained with ethidium bromide and photographed under a UV transilluminator.

High Resolution Melt Curve Analysis

Amplicons to be screened using HRM were selected according to our criteria of fragment complexity for variants previously detected using DGGE. Sample numbers were dependent on variant availability of the fragments as per previous DGGE analysis. Primers for HRM curve analysis were similarly designed using the Primer Designer computer program version 2.0 and synthesized at Integrated DNA Technology (IDT).

The PCR for HRM curve analysis using the LCGreen® PLUS DNA binding dye (Idaho Technology) was performed on an ABI thermocycler in a 10 µl reaction volume that included 10–20 ng of genomic DNA, 0.25 µM of each primer, 200 µM of each dNTP, 2 mM Mg^{2+}, 10 × PCR Buffer, 0.2 units of Hot Star Taq polymerase (QIAGEN pty Ltd, Wein, Australia) and 1 × LCGreen® PLUS DNA binding dye (Idaho Technology). PCR cycling conditions were as outlined by Idaho Technology: an initial denaturation at 95°C, followed by 45 cycles of 94°C for 30 sec and annealing for 30 sec (annealing temperatures shown in Supp. Table S1), followed by one cycle of 94°C for 30 sec and 25°C for 30 sec for heteroduplex formation. A 20 µl PCR using HRM Master Dye (Roche) was performed on the LightCycler® 480 and included approximately 10 ng of genomic DNA, 4 µM of each primer, 3 mM $MgCl_2$ and 10 µl of 1 × HRM Master dye, which includes reaction buffer, dNTP mix, FastStart Taq DNA polymerase and HRM Dye. GC-RICH solution (Roche) was added in an attempt to enhance the amplification of the GC-rich fragments by changing the melting behavior of the DNA. PCR cycling conditions were as outlined by Roche: an initial denaturation at 95°C, followed by 50 cycles of 95°C for 15 sec, annealing for 20 sec (annealing temperatures shown in Supp. Table S1), followed by an extension at 72°C for 30 sec. Following amplification, products were ramped for 1 min each at 95°C and 45°C to achieve heteroduplex formation.

The PCR products were ramped through a temperature range as outlined in Supp. Table S1, using either the 96-well formatted LightScanner® System (Idaho Technology) or the 384-well formatted LightCycler® 480 (Roche), to generate melt profiles from a change in fluorescence intensity that occurs when the product is heated. Melting data was normalized, temperature shifted, and displayed as derivative curves compared to the known wild-type samples [Dobrowolski et al., 2003, 2005; McKinney et al., 2004]. The "auto-group" function and the default sensitivity setting of the LightScanner®System Call-IT® software was applied to generate automatic genotype groups for five amplicons within the *SERPINA1*, *CXCR7*, *MBL,* and *VDR* genes. This "auto-group" function analyses the melt profiles, including melting temperature shifts and differences in the melt curve shape of each of the samples. The software uses this information to cluster samples into groups with similar melting profiles. The stringency of the auto-group function can be manipulated by either increasing or decreasing the sensitivity level on the software. Genotype grouping for the remaining five amplicons within *NPY, NKX3A, TP53,* and *HRAS*, run on the LightCycler® 480, was achieved using the default sensitivity value of 0.3 on the LightCycler® 480 Basic software.

Sanger Sequencing and Variant Confirmation

For each of the prescreening techniques described, DNA sequencing is required to determine the precise characteristics of variants detected. In this study, all aberrant DGGE banding patterns were sequenced using the Big Dye® Termination version 3.1 kit (ABI) and non-GC-clamped primers on an ABI Prism® 3100 genetic analyzer, for sequence identification and/or verification. The DNA sequence was therefore known for all samples tested using HRM analysis.

Results

In our laboratory, we have found DGGE to be a highly reliable method for mutation detection as well as low-throughput genotyping. The purpose of this study was to assess the ability of HRM curve analysis to detect variants previously identified using DGGE. Variants to be assessed were selected due to either the degree of complexity of the fragment within which they lay and/or the presence of multiple variants in close proximity. Specifically, the LightScanner® System (Idaho Technoloy) was assessed for detection of multiple variants and variants in alternate orientations, while the LightCycler® 480 (Roche) was assessed for variant detection in GC-rich fragments. The two systems will therefore be discussed separately.

Assessment of LightScanner® System (Idaho Technoloy)

Detecting multiple variants

Multiple DNA variants within three fragments from three genes, *SERPINA1, CXCR7,* and *MBL,* were identified using DGGE and further assessed using HRM curve analysis. LCGreen® PLUS and the LightScanner® System were used to determine the reliability of this method for detection of multiple variants. All variants discussed in this study were described using the HGVS nomenclature system (http://www.hgvs.org/mutnomen/). Nucleotide numbering was based on cDNA sequence with +1 as the A of the ATG initiation codon for the relevant reference sequence; dbSNP accession numbers were provided when available.

Screening the intron 1 region of *SERPINA1* using DGGE (45%–80% UF gradient) identified 12 easily distinguishable DGGE banding patterns (Fig. 1A). Direct sequencing revealed 12 different combinations of four single nucleotide polymorphisms (SNPs), c.−5+20C>T (rs1243160C>T), c.−5+24A>G (rs2854254A>G), c.−5+45G>T (rs6575424G>T), and a novel SNP c.−5+71G>A. Although HRM curve analysis using the LCGreen® PLUS chemistry (Idaho Technology) successfully identified all samples that were not wild type, only one of the single heterozygous combinations (c.−5+24A>G; orange curve) was distinguished, whereas the remaining 10 combinations detected on DGGE were clustered into one of two groups displayed as red and blue curves (Fig. 1B).

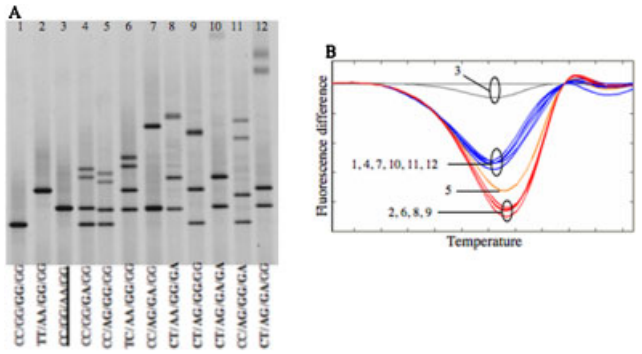

Figure 1. Multiple variants identified in the intron 1 fragment of *SERPINA1* using DGGE (**A**) and the LightScanner® System HRM curve analysis (**B**). **A:** DGGE identified 12 combinations (lanes 1 to 12) of four SNPs (c.−5+20C>T; c.−5+24A>G; c.−5+45G>T; c.−5+71G>A). The common population-specific DNA sequence is underlined (lane 3) and variants are bolded. The number of heterozygous variants present ranging from one (lanes 4, 5, and 6), two (lanes 7, 8, 9, and 11), three (lane 12) and four (lane 10) is indicated by the heteroduplex bands melting early in the gel as the number of mismatches increases. **B:** HRM differentiated the common genotype (gray curve) and one sample homozygous for the c.−5+45G>T variant and heterozygous for c.−5+24A>G (DGGE lane 5, orange curve). The remaining 10 combinations clustered into one of two groups (blue and red curves).

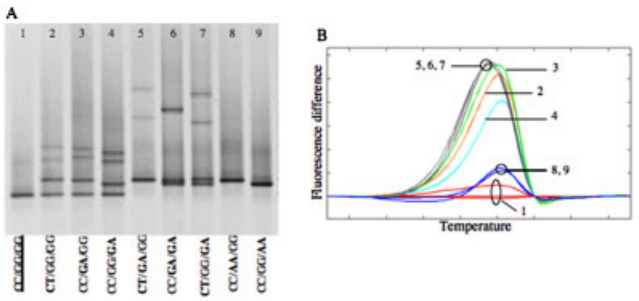

Figure 2. Detection of three commonly studied *MBL* variants in exon 2 (c.154C>T; c.161G>A; c.170G>A) using DGGE (**A**) and HRM analysis on the LightScanner® System (**B**). **A:** DGGE identified nine genotype combinations including the wild-type reference sequence (underlined), all three single heterozygous combinations (lanes 2 to 4), all three double heterozygous combinations (lanes 5 to 7), as well as homozygosity for c.161G>A (lane 8) and c.170G>A (lane 9). **B:** HRM curve analysis differentiated the wild-type (red curve) and each of the single heterozygous combinations (aqua, orange, and green curves). Samples homozygous for c.161G>A and c.170G>A variants clustered together (dark blue curve) as well as each of the double heterozygous combinations (gray curve).

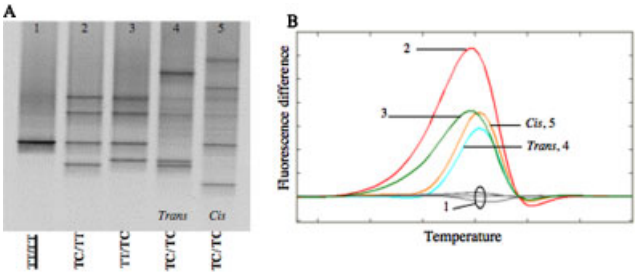

Figure 3. Detection of alternate orientations of the *SERPINA1* c.710T>C and c.840T>C variants using DGGE (**A**) and HRM analysis on the LightScanner® System (**B**). **A:** DGGE identified five genotype combinations with the wild-type allele underlined (lane 1). Two distinct DGGE banding patterns represent the *trans* (lane 4) and *cis* (lane 5) orientations of the double heterozygous combinations. **B:** HRM curve analysis successfully differentiated each of the five genotype combinations identified by DGGE, including the double heterozygous orientations (aqua and orange curves).

The region of *CXCR7* spanning exon 2, was screened using DGGE on a 45%–70% UF gradient, identifying six alternative genotype combinations (Supp. Fig. S1A). Sequencing revealed two SNPs located 108 bases apart, c.688G>A (p.Val230Ile; rs35095494G>A) and c.796C>T (p.=; rs1045879C>T). A 25% gradient of denaturants, enabled differentiation of each of the homozygous variants (lanes 2 and 3), as well as each of the heterozygous combinations (lanes 4 to 6). HRM curve analysis resulted in misclassification of the six genotype combinations into three groups (Supp. Fig. S1B). Although samples containing the double heterozygous combination (blue curve) were accurately clustered, this method repeatedly combined the two single heterozygous combinations (red curve), as well as the wild-type and two homozygous mutant combinations (gray curve).

Exon 1 of *MBL* contains three commonly studied SNPs, c.154C>T (p.Arg52Cys; rs5030737C>T), c.161G>A (p.Gly54Asp; rs1800450G>A) and c.170G>A (p.Gly57Glu; rs1800451G>A), located within a six-codon region. The close proximity of these SNPs often makes them difficult to genotype. Using DGGE (40%–70% UF gradient), nine genotype combinations were detected (Fig. 2A), compared to six combinations detected using HRM curve analysis (Fig. 2B). In this scenario, HRM accurately distinguished the three independent SNPs (orange, green, and aqua curves), but constantly failed to differentiate between the three double heterozygous combinations (gray curves) and the homozygous codon 54 and codon 57 mutants (blue curves). Of the 313 samples screened on DGGE, no individuals homozygous for codon 52 or heterozygous for all three codons were detected.

Detecting cis and trans variant orientation

Recombination events may result in mutations occurring in alternate orientations. The *SERPINA1* exon 3 amplicon was found to contain two SNPs, c.710T>C (p.Val237Ala; rs6647T>A) and c.840T>C (p.=; rs1049800T>A), occurring in both *cis* and *trans* orientation. These alternate orientations were represented on DGGE (45%–65% UF gradient) as two easily distinguishable gel-banding patterns (lanes 4 and 5; Fig. 3A). As direct Sanger sequencing is not allele specific, variant orientation was determined by gel extraction and sequencing of the DGGE homoduplex bands. In this scenario, HRM curve analysis (Fig. 3B) was successful in distinguishing variant specific heterozygosity (red and green curves) and also importantly, the two alternate *cis* (orange curve) and *trans* (aqua curve) orientations.

In a second example, two *VDR* SNPs c.2T>C (p.Met1?; rs10735810T>A) and c.146+8C>T (rs10783218C>T), were detected in both *cis* (lane 1) and *trans* (lane 2) orientation using DGGE (Supp. Fig. S2A). HRM curve analysis (Supp. Fig. S2B), however, was unable to differentiate these alternate orientations (red curves).

Assessment of LightCycler® 480 (Roche)

Detecting variants in GC-rich fragments

Sequence analysis in GC-rich regions has proven problematic for almost all variant detection methods. We assessed the capability of HRM curve analysis using the LightCycler® 480 (Roche), to detect variants identified using DGGE in five GC-rich fragments of four genes, *NKX3A*, *NPY*, *TP53*, and *HRAS*, including single and multiple variants.

DGGE was used to screen for a single polymorphic variant of *NKX3A*, c.154C>T (p.Arg52Cys; rs2228013C>T), using a 60%–80% UF gradient and 7.5-hr electrophoresis at 150 V (Fig. 4A). This region is classified as GC-rich containing 72.5% GC nucleotides. Initial HRM curve analysis did not clearly distinguish between wild-type and heterozygous genotypes with large replication error rates (Fig. 4B). Addition of GC-RICH solution (Fig. 4C), however, did improve analysis such that the heterozygous genotypes now formed a single cluster (red curve), whereas homozygous mutant samples grouped with the wild-type (blue curves).

The detection of the rarer c.20T>C (p.Leu7Pro; rs16139T>C) variant in a 66% GC-rich region of *NPY* was achieved using both DGGE (Supp. Fig. S3A) and HRM curve analysis (Supp. Fig. S3C). Optimal screening conditions for DGGE was obtained using a 60%–80% UF denaturing gradient in a 9%–12% polyacrylamide gel run for 7.5 hr at 150 V. Without GC-RICH solution (Supp. Fig. S3B), HRM curve analysis of this fragment resulted in a single wild-type sample failing to group with the remaining reference samples (yellow curve). Addition of GC-RICH solution to the PCR corrected this genotyping error (Supp. Fig. S3C). No individuals homozygous for this variant were detected.

Detecting somatic variants in GC-rich fragments

Detecting mutations in DNA extracted from tumor material can often be problematic. First, samples are often contaminated with large amounts of normal tissue, diluting the total amount of somatic variation present in the amplicon. Further complicating detection, using a number of presequencing technologies, such as HRM, is a loss of heterozygosity (LOH), which will result in the variation being present as hemizygous. In this study we assessed the ability of HRM to detect somatic variations in DNA from bladder cancer tissue or cancer cell lines in GC-rich fragments from two commonly mutated cancer-related genes, *TP53* and *HRAS*.

Three variants occurring in a 66% GC-rich fragment of exon 5 in *TP53*, were detected in five combinations using DGGE on a 40%–80% UF gradient, electrophoresed at 150 V for 6 hr (Fig. 5A). Variants included, a common SNP c.524G>A (p.Arg175His; rs28934578G>A, lanes 3 and 4) and reported *TP53* mutations c.469G>T (p.Val157Phe, lane 2) and c.536A>G (p.His179Arg, lane 5). The two variants c.469G>T (lane 2) and c.524G>A (lane 3), which appear as homozygous on DGGE, represent a hemizygous state due to LOH. HRM curve analysis without GC-RICH solution grouped all homozygous and hemizygous variants together (blue curves). Although the two heterozygous variants (c.524G>A and c.536A>G) appear as two distinct curves on the difference plot, both were classified as a single group (red curves) using the standard sensitivity settings of the data analysis software (Fig. 5B). These heterozygous curves and the hemizygous c.469G>T variant were grouped separately after increasing the sensitivity to 0.75 (data not shown). Addition of GC-RICH solution (Fig. 5C) resulted in each of the heterozygous variants being grouped separately (red and green curves), whereas homozygous and hemizygous variants were grouped together (blue curves).

A second *TP53* fragment in exon 4, consisting of 65% GC nucleotides, was screened for somatic variation using DGGE on a 40%–80% UF gradient at 150 V for 7 hr (Supp. Fig. S4A). Analysis of 25 samples resulted in six distinct banding patterns as a result of four variants, c.215C>G (p.Pro72Arg; rs1042522C>G), a G>T transversion c.313G>T (p.Gly105Cys), a 1-bp deletion, c.211del (c.211delC) occurring at the first base of

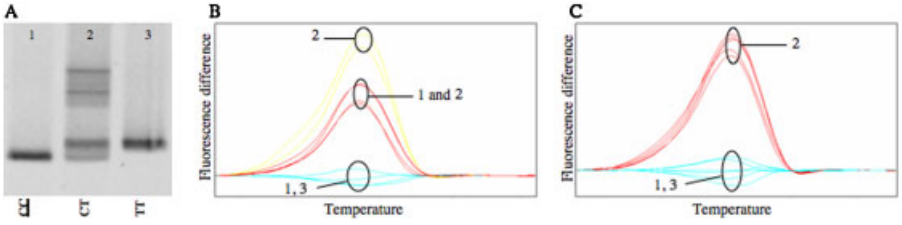

Figure 4. Detection of a single variant c.154C>T in a 72.5% GC rich region of *NKX3A* using DGGE (**A**) and HRM curve analysis on the LightCycler® 480 without (**B**) and with (**C**) GC-RICH solution. **A:** DGGE analysis of this fragment resulted in three distinct banding patterns representing the wild-type (lane 1), heterozygous (lane 2) and homozygous mutant (lane 3) genotypes. **B:** Without GC-RICH solution, HRM analysis resulted in three clusters, one consisting of a combination of wild-type and heterozygous samples (red curves). **C:** Addition of GC-RICH solution to the HRM PCR eliminates this third cluster such that two groups are formed, wild-type and homozygous mutant (blue curves) and heterozygous samples (red curves).

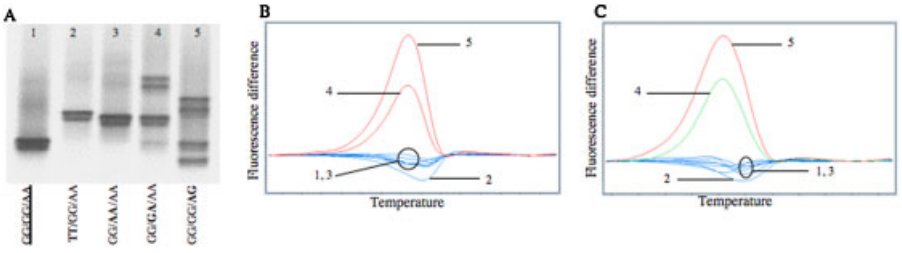

Figure 5. Multiple variants identified in a 66% GC rich fragment in exon 5 of *TP53* using DGGE (**A**) and HRM curve analysis on the Roche LightCycler® 480 without (**B**) and with (**C**) GC-RICH solution. **A:** DGGE identified five combinations of three variants (c.469G>T; c.524G>A; c.536A>G), including two hemizygous mutants for each c.469G>T (lane 2) and c.524G>A (lane 3) variants as well as samples heterozygous for either c.524G>A (lane 4) or c.536A>G (lane 5). **B:** HRM curve analysis without GC-RICH solution did not differentiate between the two single heterozygous variants (red curves) or between the wild-type and hemizygous combinations using the software's default analysis settings. **C:** Addition of GC-RICH solution resulted in the two single heterozygous variants being grouped separately.

codon 71 (p.Pro71fs) and a novel 26 bp deletion, c.261_286del (c.261_286delAGCCCCCTCCTGGCCCCTGTCATCTT) extending from the last base of codon 87 to the first base of codon 96 (p.Pro87fs). HRM curve analysis of this amplicon was not optimal, as the fragment appeared to contain two melting transitions clearly evident on the normalized melt curves (data not shown) and on the difference plots (Supp. Fig. S4B and S4C). Optimal placement of the GC-rich clamp during DGGE primer design allows for a single melting domain and thus optimal mutation detection across the entire amplicon. Without GC-RICH solution (Supp. Fig. S4B), each of the two samples containing a deletion were individually grouped (red and pink curves), as was the double heterozygous sample (green curve). The two single heterozygous combinations clustered with the reference curve. In this scenario, GC-RICH solution failed to improve HRM analysis for this amplicon (Supp. Fig. S4C).

A region in exon 2 of *HRAS*, containing 65% GC content, and covering the hotspot oncogenic region, was screened on DGGE using a 45%–75% UF gradient, electrophoresed for 7 hr at 150 V (Supp. Fig. S5A). Seven distinct banding patterns were observed for 14 samples as a result of four variants. These included c.81T>C (p.=; rs12628T>A, lane 5), a C>T substitution 5′ of the translation start site, c.−10C>T (lane 7) and two oncogenic mutations occurring at a single nucleotide position in codon 12, c.35G>A (p.Gly12Asp, lane 2) and c.35G>T (p.Gly12Val, lane 3). Hemizygous mutations due to LOH, were detected for variants c.35G>T (lane 4) and c.81T>C (lane 6). Using HRM curve analysis without GC-RICH solution (Supp. Fig. S5B), c.−10C>T and c.35G>T heterozygous variants were grouped (red curves), heterozygous variants c.81T>C and c.35G>A clustered with the wild-type (blue curves), and hemizygous variants c.35G>T and c.81T>C grouped together (green curves). The addition of GC-RICH solution did not improve the distinction of variants within this fragment (Supp. Fig. S5C).

Discussion

The purpose of this study is not a direct comparison of the DGGE and HRM methods, but rather to assess the capability of the HRM method to detect multiple, often complex, combinations of DNA variants occurring in single amplicons previously detected using DGGE. Both HRM and DGGE methods are based on DNA melt profiling. Therefore, we aimed to determine (if any) potential advantages and/or limitations of the HRM method of particular note for clinical laboratories planning to adopt this new technique. Several studies have reported on the high sensitivity, ease of data interpretation, and the low cost associated with using DGGE for detecting DNA sequence variation [Hayes, 2003; Macek et al., 1997; Petersen et al., 2002; van der Hout et al., 2006]. Depending on the enzyme used for amplification, the cost of reagents to perform DGGE screening is a half to three-quarter that required for HRM using these platforms and dyes. Despite these advantages, DGGE and other gel-based methods are gradually and unavoidably being replaced by more high-throughput methods such as HRM curve analysis, requiring less technical expertise and hands-on time, as well as excluding hazardous substances required such as polyacrylamide, formamide, and TEMED used in DGGE. These new methods, however, require extensive and comprehensive validation before replacing current diagnostic techniques.

Many of the DNA variants within gene regions assessed in this study have the potential to influence susceptibility and/or progression of disease [Aoki et al., 2005; Cicek et al., 2006; Hayes and Gardiner-Garden, 2003; Petitjean et al., 2007; Rodriguez Ortner et al., 2006; Skibola et al., 2005; Wang et al., 2008], and therefore their detection may have clinical relevance. Although HRM curve analysis has been tested and shown to be successful in a number of research laboratories for clinical use [Chou et al., 2005; Dobrowolski et al., 2005, 2007a, 2007b; Grievink and Stowell, 2008; Kennerson et al., 2007; Krypuy et al., 2006; Lonie et al., 2006; Margraf et al., 2006; Poláková et al., 2008; Seipp et al., 2008; Smith et al., 2008; Willmore-Payne et al., 2006], we wanted to assess this method for detecting multiple sequence variants, as well as single and multiple variants (including both constitutional and somatic), within GC-rich fragments, as it would be applied in a diagnostic setting, with minimal expertise and time to manipulate assay design. This was achieved by screening five fragments for 13 variants in a total of 35 different combinations using the LightScanner® System and LC Green® PLUS DNA binding dye (Idaho Technology) as well as screening five GC-rich (≥65%) fragments for 12 variants in 22 combinations using the LightCycler® 480 and HRM Master dye (Roche).

In each of the scenarios tested, fragment sizes were no more than 353 bases in length (excluding GC-clamp for DGGE amplicons) and each contained one to four variants between zero and 152 bp apart. The variants were present in a variety of combinations, including *cis* and *trans* orientation, as well as alleles at the same nucleotide position and single or multiple bp deletions. Variants were predominantly C>T or G>A transitions, the most common type of genetic variation that occurs in the human genome [Rosenberg et al., 2003]. Both DGGE and HRM curve analysis are genetic screening methods based on amplicon melt temperature. One limitation of such methods is that the T_m may not differ sufficiently between two alleles to differentiate the variants, particularly for neutral bp changes (e.g., A>T, T>A, or C>G, G>C) [von Ahsen et al., 2001]. As the scenarios tested in this study were predominantly of nonneutral changes (commonly C>T and G>A transitions), this factor should not have influenced our results.

The ability to screen fragments containing more than one variant is not only beneficial in terms of time and cost, but often unavoidable when variants are closely located. Detection of multiple variants using Idaho Technology's LC Green® PLUS DNA binding dye and the high-resolution melting instrument has been reported previously, including three SNPs in six combinations [Wittwer et al., 2003] and four SNPs in seven combinations [Graham et al., 2005]. Our assessment of this technology to detect multiple variants revealed important limitations. This was not only apparent for the identification of known variants, such as reported SNPs or known causative mutations assessed in diagnostic laboratories, but also introduced the potential of either missing or misclassifying novel sequence variants.

For the unique application of differentiating between variants in *cis* and *trans* orientation, HRM curve analysis was successful for one (*SERPINA1*, exon 3) of the two fragments. Determining variant orientation is particularly important in cases where functional variants may have differing biological effects depending on their orientation. As Sanger sequencing is unable to detect allele specific orientation, both DGGE and HRM curve analysis show this added advantage to using a presequencing technique. One must caution, however, that HRM curve analysis did not differentiate between alternate orientations in both scenarios tested for this study.

GC-rich regions have proven an obstacle for most genetic screening methods, including Sanger sequencing, and particularly those that use temperature shifts to detect sequence variation. Previous reports have shown that DGGE run at optimised conditions can be a highly sensitive tool for such fragments

[Hayes et al., 1999; Lacerra et al., 2004; Wu et al., 1999], and is therefore an appropriate platform for assessing new methods for this application. One report, which discusses HRM curve analysis of GC-rich fragments [Reed and Wittwer, 2004], suggests that GC content has no effect on HRM curve analysis, and also that biphasic melting curves may be easier to analyze than those with a single melt domain. This report is in conflict with other studies that suggest GC-rich regions and multiple melting domains should be avoided for HRM curve analysis [Krypuy et al., 2007].

Using the LightCycler® 480 and HRM Master dye (Roche), our results indicate that for single SNP analysis in GC-rich fragments, including a 72.5% and 66% GC-rich region in *NKX3A* and *NPY,* respectively, the addition of GC-RICH solution (Roche) to the PCR may assist in correctly grouping samples on HRM curve analysis. For GC-rich fragments that contain multiple variants, the GC-RICH solution had varied effects, with only one (*TP53*, exon 5) of the three fragments tested showing improved results. We would therefore recommend that fragments be tested with and without GC-RICH solution during assay optimisation for HRM curve analysis.

An additional concern highlighted in this study is the analysis of somatic variants in tumor material. Many of these variants will occur as a single allelic variant due to LOH of the second allele. It is well established that both dHPLC and now HRM nongel-based methods are not well suited for detection of homozygous variants, and that spiking of samples is often the routine procedure. Although spiking may dramatically improve mutation detection rates, one must also caution that this will further dilute the mutant allele concentration in the starting sample. A previous study has demonstrated HRM analysis, able to detect as little as 5%–6% tumor cell line DNA in a background of wild-type DNA [Krypuy et al., 2006]. These investigators also report that sensitivity is likely influenced by the size and possibly the GC content of the fragment being assessed.

There are several reasons for researchers to investigate more recent methods such as HRM curve analysis for mutation detection. HRM analysis is a prescreening method aimed at improving the turn-around time, which together with the reduced technical expertise required compared to gel-based methods such as DGGE, makes this method an ideal diagnostic/clinical tool. HRM allows for melt profiles of up to 96 or 384 PCR products to be achieved in minutes, compared to at least 24 hr for most gel-based methods. Although time and technical expertise are important factors, there are several other aspects to consider prior to embracing these newer technologies. One of the more vital aspects to consider includes assay sensitivity. In this study, we demonstrate multiple mutations, previously identified using the highly sensitive DGGE method, being missed or misclassified using HRM curve analysis. Additional considerations include the recent observation that HRM analysis requires careful attention to primer design, as mutation detection is easier when there is a single melting domain [Krypuy et al., 2007], a concept highly comparable to the DGGE method [Wu et al., 1999]. The large amount of sequencing required using HRM curve analysis and spiking due to lack of sensitivity to detect homozygous or hemizygous mutations, must also be considered. The latter point is particularly important, as more laboratories use this method for genotyping of common DNA variants, thereby excluding additional sequencing. Together with a recent report of a higher failure rate and incorrect allele allocation using HRM for genoptyping, when compared to TaqMan allelic discrimination [Bass et al., 2007], diagnostic laboratories should be cautious when adopting this method of choice for this purpose. For detection of rare DNA variants, it may be argued that HRM need not distinguish DNA variants, but is rather a presequencing technique in the true sense of the word and only needs to detect that a fragment requires sequencing. This study emphasises the importance of this previous statement, concluding that melt profiles should not be used for variant classification without complementary sequence validation. Caution should therefore be applied when assumptions are made that the same melt profile equates to the same DNA sequence. An approach only recommended for well-validated HRM genotyping assays, and assuming that no other rare variants may occur within the specific amplicon. In conclusion, laboratories intending to embrace this new method should invest significant effort in understanding its limitations and in assay optimisation, to achieve its full potential without compromising on the high degree of sensitivity required for diagnostic testing.

Acknowledgments

We thank Ms. Emma Carr for her contribution to sample processing. Grant support was provided by Cancer Institute of New South Wales (V.M.H. is a Fellow, E.A.T. is a PhD Scholar), Australian Rotary Health Research Foundation (E.A.T. is a PhD Scholar), and the Freeman Foundation, Australia (D.C.P. was a Postdoctoral Fellow).

References

Abrams ES, Murdaugh SE, Lerman LS. 1990. Comprehensive detection of single base changes in human genomic DNA using denaturing gradient gel electrophoresis and a GC clamp. Genomics 7:463–475.

Aoki Y, Niihori T, Kawame H, Kurosawa K, Ohashi H, Tanaka Y, Filocamo M, Kato K, Suzuki Y, Kure S, Matsubara Y. 2005. Germline mutations in HRAS proto-oncogene cause Costello syndrome. Nat Genet 37:1038–1040.

Bass C, Nikou D, Donnelly MJ, Williamson MS, Ranson H, Ball A, Vontas J, Field LM. 2007. Detection of knockdown resistance (*kdr*) mutations in Anopheles gambiae: a comparison of two new high-throughput assays with existing methods. Malar J 13:111–124.

Bentley DR. 2006. Whole-genome re-sequencing. Curr Opin Genet Dev 16:545–552.

Chou LS, Lyon E, Wittwer CT. 2005. A comparison of high-resolution melting analysis with denaturing high performance liquid chromatography for mutation scanning. Am J Clin Pathol 124:330–338.

Cicek MS, Liu X, Schumacher FR, Casey G, Witte JS. 2006. Vitamin D receptor genotypes/haplotypes and prostate cancer risk. Cancer Epidemiol Biomarkers Prev 15:2549–2552.

Cotton RGH, Rodrigues NR, Campbell RD. 1988. Reactivity of cytosine and thymine in single-base-pair mismatches with hydroxylamine and osmium tetroxide and its application to the study of mutations. Proc Natl Acad Sci USA 85:4397–4401.

Dobrowolski SF, Longo N, McKinney JT. 2003. Mutation screening in primary carnitine deficiency using LC green and high resolution thermal denaturation. J Inherit Metab Dis 26:S188.

Dobrowolski SF, McKinney JT, Amat di San Filippo C, Giac Sim K, Wilken B, Longo N. 2005. Validation of dye-binding/high-resolution thermal denaturation for the identification of mutations in the SLC22A5 gene. Hum Mutat 25:306–313.

Dobrowolski SF, Ellingson CE, Caldovic L, Tuchman M. 2007a. Streamlined assessment of gene variants by high resolution melt profiling utilizing the ornithine transcarbamylase gene as a model system. Hum Mutat 28:1133–1140.

Dobrowolski SF, Ellingson C, Coyne T, Grey J, Martin R, Naylor EW, Koch R, Levy HL. 2007b. Mutations in the phenylalanine hydroxylase gene identified in 95 patients with phenylketonuria using novel systems of mutation scanning and specific genotyping based upon thermal melt profiles. Mol Genet Metab 91:218–227.

Fischer SG, Lerman LS. 1983. DNA fragments differing by single base-pair substitutions are separated in denaturing gradient gels: correspondence with melting theory. Proc Natl Acad Sci USA 80:1579–1583.

Ganguly A, Rock MJ, Prockop DJ. 1993. Confirmation-sensitive gel electrophoresis for rapid detectopn of single-base differences in double-stranded PCR products and DNA fragments: evidence for solvent-induced bends in DNA heteroduplexes. Proc Natl Acad Sci USA 90:10325–10329.

Graham R, Liew M, Meadows C, Lyon E, Wittwer CT. 2005. Distinguishing different DNA heterozygous by high-resolution melting. Clin Chem 51:1295–1298.

Grievink H, Stowell KM. 2008. Identification of ryanodine receptor 1 single-nucleotide polymorphisms by high-resolution melting using the LightCycler 480 system. Anal Biochem 374:396–404.

Hayes VM, Wu Y, Osinga J, Mulder IM, van der Vlies P, Elfferich P, Buys CHCM, Hofstra RMW. 1999. Improvements in gel composition and electrophoretic conditions for broad-range mutation analysis by denaturing gradient gel electrophoresis. Nucleic Acids Res 27:e29.

Hayes VM. 2003. Alpha-1-Antitrypsin gene in Africans identified using a novel genotyping assay. Hum Mutat 22:59–66.

Hayes VM, Gardiner-Garden M. 2003. Are polymorphic markers within the α-1-Antitrypsin gene associated with risk of human immunodeficiency virus disease? Am J Infect Dis 188:1205–1208.

Hayes VM, Severi G, Padilla EJD, Eggleton SA, Southey MC, Sutherland RL, Hopper JL, Giles GG. 2005. Haplotype associations of vitamin D receptor polymorphisms do not contribute to risk of prostate cancer. Cancer Epidemiol Biomarkers Prev 14:997–999.

Highsmith WE, Nataraj AJ, Jin Q, O'Connor JM, El-Nabi SH, Kusukawa N, Garner MM. 1999. Use of DNA toolbox for the characterization of mutation scanning methods: II. Evaluation of single-strand confirmation polymorphism analysis. Electrophoresis 20:1195–1203.

Kennerson ML, Warburton T, Nelis E, Brewer M, Polly P, De Jonghe P, Timmerman V, Nicholson GA. 2007. Mutation scanning the *GJB1* gene with high-resolution melting analysis: implications for mutation scanning of genes for Charcot-Marie-Tooth disease. Clin Chem 53:349–352.

Krypuy M, Newnham GM, Thomas DM, Conron M, Dobrovic A. 2006. High resolution melting analysis for the rapid and sensitive detection of mutations in clinical samples: *KRAS* codon 12 and 13 mutations in non-small cell lung cancer. BMC Cancer 6:295–306.

Krypuy M, Ahmed AA, Etemadmoghadam D, Hyland SJ, Australian ovarian cancer study group, deFazio A, Fox SB, Brenton JD, Bowtell DD, Dobrovic A. 2007. High resolution melting for mutation scanning of *TP53* exons 5-8. BMC Cancer 7:168–180.

Lacerra G, Fiorito M, Musollino G, Di Noce F, Esposito M, Nigro V, Gaudiano C, Carestia C. 2004. Sequence variations of the α-Globin genes: scanning of high CG content genes with DHPLC and DG-DGGE. Hum Mutat 24:338–349.

Laurie AD, Smith MP, George PM. 2007. Detection of factor VIII gene mutations by high resolution melting analysis. Clin Chem 53:2211–2214.

Lerman LS, Silverstein K. 1987. Computational simulation of DNA melting and its application to denaturing gradient gel electrophoresis. Methods Enzymol 155:482–501.

Lonie L, Porter DE, Fraser M, Cole T, Wise C, Yates L, Wakeling E, Blair E, Morava E, Monaco AP, Ragoussis J. 2006. Determination of the mutation spectrum of the *EXT1*/*EXT2* genes in British Caucasian patients with multiple osteochondromas, and exclusion of six genes in *EXT* negative cases. Hum Mutat 27:1160.

Macek Jr M, Mercier B, Macková A, Weiner Miller P, Hamosh A, Férec C, Cutting GR. 1997. Sensitivity of the denaturing gradient gel electrophoresis techniques in detection of known mutations and novel Asian mutations in the *CFTR* gene. Hum Mutat 9:136–147.

Margraf RL, Mao R, Highsmith WE, Holtegaard LM, Wittwer CT. 2006. Mutation scanning of the *RET* protooncogene using high-resolution melting analysis. Clin Chem 52:138–141.

Margulies M, Egholm M, Altman WE, Attiya S, Bader JS, Bemben LA, Berka J, Braverman MS, Chen Y, Chen Z, Dewell SB, Du L, Fierro JM, Gomes XV, Godwin BC, He W, Helgesen S, He Ho C, Irzyk GP, Jando SC, Alenquer MLI, Jarvie TP, Jirage KB, Kim JB, Knight JR, Lanza JR, Leamon JH, Lefkowitz SM, Lei M, Li J, Lohman KL, Lu H, Makhijani VB, McDade KE, McKenna MP, Myers EW, Nickerson E, Nobile JR, Plant R, Puc BP, Ronan MT, Roth GT, Sarkis GJ, Simons JF, Simpson, JW, Srinivasan M, Tartaro KR, Tomasz A, Vogt KAVolkmer GA, Wang SH, Wang Y, Weiner MP, Yu P, Begley RF, Rothberg JM. 2005. Genome sequencing in microfabricated high-density picolitre reactors. Nature 437:376–380.

McKinney JT, Longo N, Hahn SH, Matern D, Rinaldo P, Strauss AW, Dobrowlski SF. 2004. Rapid, comprehensive screening of the human medium chain acyl-CoA dehydrogenase gene. Mol Genet Metab 82:112–120.

Myers RM, Larin Z, Maniatis T. 1985. Detection of single base substitutions by ribonuclease cleavage at mismatches in RNA:DNA duplexes. Science 230:1242–1246.

Myers RM, Maniatis T, Lerman LS. 1987. Detection and localization of single base changes by denaturing gradient gel electrophoresis. Methods Enzymol 155:501–527.

Orita M, Iwahana H, Kanazawa H, Hayashi K, Sekiya T. 1989. Detection of polymorphisms of human DNA by gel electrophoresis as single-stranded conformation polymorphisms. Proc Natl Acad Sci USA 86:2766–2770.

Papp AC, Pinsonneault JK, Cooke G, Sadée W. 2003. Single nucleotide polymorphism genotyping using allele-specific PCR and fluorescence melting curves. BioTechniques 34:1068–1072.

Petersen DC, Laten A, Zeier MD, Grimwood A, van Rensburg EJ, Hayes VM. 2002. Novel mutations and SNPs identified in *CCR2* using a new comprehensive denaturing gradient gel electrophoresis assay. Hum Mutat 20: 253–259.

Petitjean A, Mathe E, Kato S, Ishioka C, Tavtigian SV, Hainaut P, Olivier M. 2007. Impact of mutant p53 functional properties on TP53 mutation patterns and tumor phenotype: lessons from recent developments in the IARC TP53 database. Hum Mutat 28:622–629.

Poláková KM, Lopotová T, Klamová H, Moravcová J. 2008. High Resolution melt curve analysis: initial screening for mutations in BCR-ABL kinase domain. Leuk Res 32:1236–1243.

Reed GH, Wittwer CT. 2004. Sensitivity and specificity of single-nucleotide polymorphism scanning by high-resolution melting analysis. Clin Chem 50:1748–1754.

Ririe KM, Rasmussen RP, Wittwer CT. 1997. Product differentiation by analysis of DNA melting curves during the polymerase reaction. Anal Biochem 245:154–160.

Rodriguez Ortner E, Hayes RB, Weissfeld J, Gelmann EP. 2006. Effect of homeodomain protein NKX3.1 R52C polymorphism on prostate gland size. Urology 67:311–315.

Rosenbaum V, Riesner D. 1987. Temperature-gradient gel electrophoresis: thermodynamic analysis of nucleic acids and proteins in purified form and in cellular extracts. Biophys Chem 26:235–246.

Rosenberg MS, Subramanian S, Kumar S. 2003. Patterns of transitional mutation biases within and among mammalian genomes. Mol Biol Evol 20:988–993.

Schuster SC. 2008. Next-generation sequencing transforms today's biology. Nat Methods 5:16–18.

Seipp MT, Pattison D, Durtschi JD, Jama M, Voelkerding KV, Wittwer CT. 2008. Quadruplex genotyping of F5, F2, and *MTHFR* variants in a single closed tube by high-resolution amplicon melting. Clin Chem 54: 108–115.

Sheffield VC, Cox DR, Lerman LS, Myers RM. 1989. Attachment of a 40-base-pair G + C-rich sequence (GC-clamp) to genomic DNA fragments by the polymerase chain reaction results in improved detection of single-base changes. Proc Natl Acad Sci USA 86:232–236.

Skibola DR, Smith MT, Bracci PM, Hubbard AE, Agana L, Chi S, Holly EA. 2005. Polymorphisms in Ghrelin and Neuropeptide Y genes are associated with non-Hodgkin lymphoma. Cancer Epidemiol Biomarkers Prev 14: 1251–1256.

Smith GD, Chadwick BE, Willmore-Payne C, Bentz JS. 2008. Detection of epidermal growth factor receptor gene mutations in cytology specimens from patients with non-small cell lung cancer utilising high-resolution melting amplicon analysis. J Clin Pathol 61:487–493.

van der Hout AH, van den Ouweland AMW, van der Luijt RB, Gille HJP, Bodmer D, Brüggenwirth H, Mulder IM, van der Vlies P, Elfferich P, Huisman MT, ten Berge AM, Kromosoeto J, Jansen RPM, van Zon PHA, Vriesman T, Arts N, Boutmy-de Lange M, Oosterwijk JC, Meijers-Heijboer H, Ausems MGEM, Hoogerbrugge N, Verhoef S, Halley DJJ, Vos YJ, Hogervorst F, Lightenberg M, Hofstra RMW. 2006. A DGGE system for comprehensive mutation screening of *BRCA1* and *BRCA2*: application in a Dutch cancer clinic setting. Hum Mutat 27:654–666.

Von Ahsen N, Oellerich M, Schütz E. 2001. Limitations of genotyping based on amplicon melt temperature. Clin Chem 47:1331–1332.

Wang FY, Tahara T, Arisawa T, Shibata T, Yamashita H, Nakamura M, Yoshioka D, Okubo M, Maruyama N, Kamano T, Kamiya Y, Nakamura M, Fujita H, Nagasaka M, Iwata M, Takahama K, Watanabe M, Nakano H, Hirata I. 2008. Mannan-binding lectin (MBL) polymorphism and gastric cancer risk in Japanese population. Dig Dis Sci 52:1691–1697.

Willmore-Payne C, Holden JA, Chadwick BE, Layfield LJ. 2006. Detection of *c-kit* exons 11- and 17-activating mutations in testicular seminomas by high-resolution melting amplicon analysis. Mod Pathol 19:1164–1169.

Wittwer CT, Reed GH, Gundry CN, Vandersteen JG, Pryor RJ. 2003. High-resolution genotyping by amplicon melting analysis using LCGreen. Clin Chem 49:853–860.

Wu Y, Hayes VM, Osinga J, Mulder IM, Looman MWG, Buys CHCM, Hofstra RMW. 1998. Improvement of fragment and primer selection for mutation detection by denaturing gradient gel electrophoresis. Nucleic Acids Res 26: 5432–5440.

Wu Y, Stulp RP, Elfferich P, Osinga J, Buys CHCM, Hofstra RMW. 1999. Improved mutation detection in GC-rich DNA fragments by combined DGGE and CDGE. Nucleic Acids Res 27:e9i–iii.

Xiao W, Oefner PJ. 2001. Denaturing high-performance liquid chromatography: a review. Hum Mutat 17:439–474.